Journal of Science and Transport Technology
Journal homepage: https://jstt.vn/index.php/en

Efficient Structural Analysis: Predicting Punching Shear Strength in Two-Way Concrete Slabs Using Gradient Boosting Machine Learning

Lam Huu Quang[1], Gia Linh Bui[2], Thuy-Anh Nguyen[2,*]
[1]Institute of Transport Science and Technology, 1252 Lang Street, Hanoi 100000, Viet Nam
[2]University of Transport Technology, 54 Trieu Khuc, Thanh Xuan, Hanoi 100000, Vietnam

Article info
Type of article:
Original research paper

DOI:
https://doi.org/10.58845/jstt.utt.2024.en.4.1.42-57

***Corresponding author:**
E-mail address:
anhnt@utt.edu.vn

Received: 06/03/2024
Revised: 30/03/2024
Accepted: 30/03/2024

Abstract: This study delves into the application of machine learning (ML), specifically a Gradient Boosting (GB) model, for predicting the punching shear strength (PSS) of two-way reinforced concrete flat slabs. Leveraging a dataset comprising 241 experimental observations from reputable sources, the research investigates the influence of critical factors on PSS, including slab thickness, column section width, effective slab depth, reinforcement ratio, concrete compressive strength, and reinforcement yield strength. Hyperparameter optimization techniques are employed to fine-tune the model's parameters, leading to enhanced predictive performance. Monte Carlo simulations are utilized to validate the model's reliability and generalizability. The results demonstrate that the GB model achieves high precision and reliability, reducing the need for resource-intensive experimentation in predicting PSS for two-way slabs. Furthermore, the study compares the performance of the developed model with that of conventional design codes, highlighting the model's superior accuracy. This research contributes to the broader application of ML in structural engineering, offering an efficient and accurate approach to analyzing and designing structural elements.

Keywords: Machine Learning; Punching shear strength (PSS), Two-way slab.

1. Introduction

Two-way slabs constitute a prevalent structural component widely employed in the construction of buildings, owing to their adaptability and robust load-bearing capabilities. These slabs are pivotal in sustaining diverse structures and efficiently disseminating loads in both horizontal directions. An essential mechanical attribute profoundly impacting the performance of two-way slabs relates to their capacity for withstanding punching shear forces. It is noteworthy that punching shear failures occur abruptly and can potentially result in the gradual deterioration of the overall structural integrity [1]. Investigating punching shear resistance in two-way slabs yields critical insights into their structural behavior. Analyzing the results, it becomes evident that a thorough comprehension of punching shear mechanisms is imperative for ensuring the safety and stability of building structures.

Punching shear strength (PSS), a critical parameter in the structural analysis of two-way

labs, refers to the capacity of the slab to withstand concentrated forces around columns or other load-bearing elements. However, the determination of PSS proves to be a challenging task owing to its susceptibility to various associated factors. To address this challenge, extensive experimental research has been undertaken to identify the key factors influencing PSS. Notably, studies conducted by Elstner and Hognestad [2], Moe [3], Mowrer and Vanderbilt [4], Regan [5], and Guandalini et al. [6] have been instrumental in this regard. These investigations focus on understanding the impact of parameters such as column size, slab dimensions, concrete compressive strength, yield strength of reinforcement, reinforcement ratio, and loading conditions on the punching shear failure of reinforced concrete slabs. In addition to illuminating the behavior of reinforced concrete slabs under punching shear forces, these testing programs furnish invaluable datasets for ongoing research endeavors, aiding in developing and validating new models. This body of research continues to play a crucial role in enhancing our comprehension of PSS and advancing structural engineering practices.

Furthermore, numerous design codes, including ACI 318-08 [7], BS-8110-97 [8], CEB-FIP-90 [9], and Euro-Code 2 [10], present empirical equations aimed at forecasting the PSS of two-way reinforced concrete slabs. Although these equations typically offer user-friendly solutions with restricted parameters, it is crucial to recognize that most of them rely on empirical methodologies derived from experimental data during their development. As a result, the outcomes generated by these equations for the same structural scenario often exhibit disparities, and some require additional assistance in accurately ascertaining the PSS of two-way reinforced concrete slabs. In conclusion, while empirical equations found in design codes offer practical tools for estimating PSS in two-way reinforced concrete slabs, their empirical nature leads to variations in results. Engineers must exercise caution when utilizing these equations and consider the unique characteristics of their structural systems. Furthermore, there is a pressing need for further research to refine and expand our understanding of PSS mechanisms, leading to more accurate and consistent predictions in structural engineering practice.

In recent decades, artificial intelligence (AI) and machine learning (ML) have gained substantial prominence and found widespread applications across various engineering disciplines [11]-[13]. The construction industry, in particular, has harnessed ML techniques effectively [14,15]. AI models have addressed numerous intricate challenges within civil engineering, spanning fields like structural engineering [16],[17], materials science [18,19], geotechnical engineering [20,21], and earth sciences [22,23]. Notably interesting in structural design is the prediction of PSS in two-way flat slabs. In a study conducted by Hoang [24], an artificial neural network model and sequential partial linear regression were employed to estimate the PSS of fiber-reinforced concrete slabs. The findings reveal that both models surpass other experimental design equations in PSS prediction. Elshafey et al. [25] also employed an artificial neural network approach to examine the influence of concrete strength, steel reinforcement ratio, and effective depth of the slab on PSS. However, the stability and robustness of the models developed in these investigations remain unverified. These findings carry significant implications for structural engineering practice, as they suggest the potential for more accurate and reliable predictions of PSS in concrete slabs through AI and ML approaches. Nevertheless, rigorous validation and further research to enhance model stability remain critical.

In pursuit of overcoming the constraints observed in prior investigations, the primary objective of this study is to construct a ML model, specifically a Gradient Boosting (GB) model, to

predict punching shear resistance in two-way flat slabs. This model leverages a dataset of 241 experimental outcomes from respected scholarly journals. This study incorporates cross-validation and Monte Carlo simulation techniques to ensure robust model assessment and a comprehensive grasp of its stability across diverse scenarios.

2. Database description and analysis

A dataset consisting of 241 experimental observations on the PSS of two-way reinforced concrete flat slabs was collected for this research from a variety of literature sources [2],[4],[26]-[30]. The analysis of these experimental results highlights the substantial influence of several pivotal factors on the PSS of two-way reinforced concrete slabs. These factors encompass the thickness of the slab, the width of the column section, the effective depth of the slab, the reinforcement ratio, the compressive strength of concrete, and the yield strength of reinforcement. Consequently, these identified factors serve as the basis for developing ML models to predict the PSS of two-way reinforced concrete slabs.

The dataset encompasses a range of values for each parameter: slab thickness (h) ranging from 46.0 to 550.0 mm, width of column section (C) ranging from 80.0 to 520.0 mm, effective depth of slab (d) ranging from 35.0 to 500.0 mm, reinforcement ratio (rho) ranging from 0.25 to 5.01%, compressive strength of concrete (f_c) ranging from 12.3 to 119.0 MPa, and yield strength of steel (f_y) ranging from 294.0 to 720.0 MPa. The test specimens include square and circular columns, excluding those cast with lightweight concrete. They consist of reinforced concrete flat slab-column connections without drop panels, column capitals, or shear reinforcement.

Table 1 presents the statistical parameters summarizing the characteristics of the variables in the database, and the distribution of each parameter is illustrated in Fig. 1. Furthermore, the correlation matrix plot in Fig. 2 showcases the relationship between PSS and the six input parameters. This plot visually represents the pairwise correlations between parameters, each associated with its corresponding correlation coefficient. It is evident that parameters such as h, C, d, and f_c exhibit a high correlation with PSS, while parameters rho and f_y demonstrate a lower correlation with PSS.

Table 1. The input and output parameters used in the development of ML models

Parameter	Symbol	Unit	Mean	Std	Min	Median	Max
Input							
Slab thickness	h	mm	149.93	79.64	46.00	150.00	550.00
Width of the column section	C	mm	198.54	78.13	80.00	200.00	520.00
Effective depth of the slab	d	mm	121.09	70.43	35.00	114.00	500.00
Reinforcement ratio	rho	%	1.23	0.77	0.25	1.06	5.01
Compressive strength of concrete	f_c	MPa	40.70	22.75	12.30	31.50	119.00
Yield strength of steel	f_y	MPa	478.39	97.34	294.00	480.00	720.00
Output							
Punching shear strength	PSS	kN	452.92	495.80	29.00	312.00	2681.00

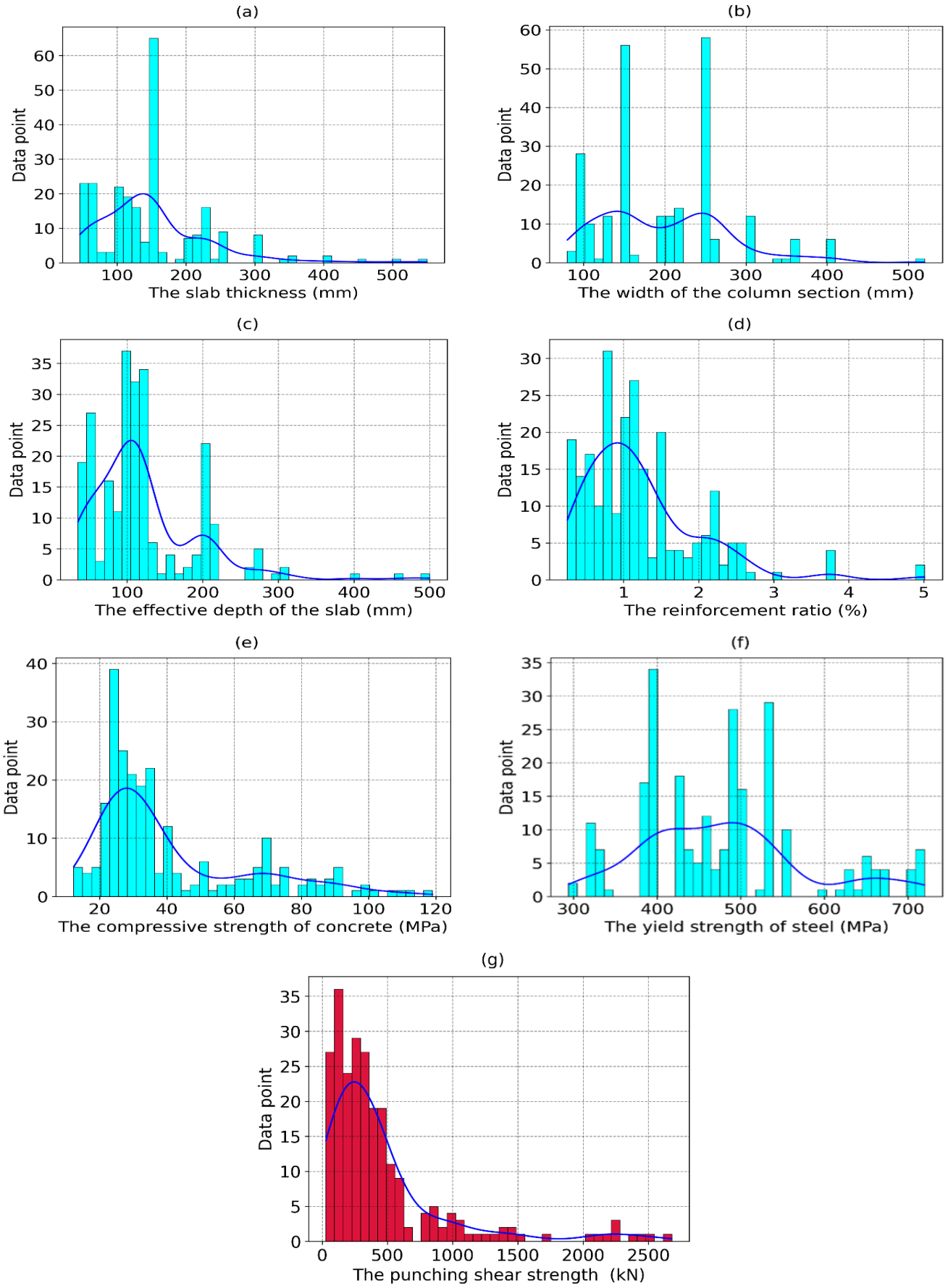

Fig. 1. Distribution of input and output parameters of the PSS data set

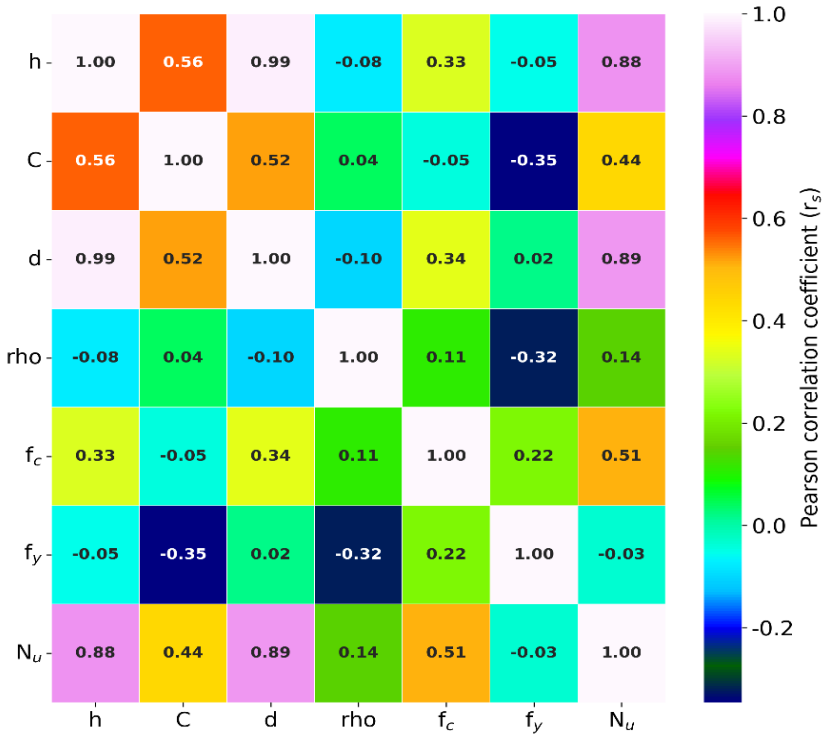

Fig. 2. Correlation matrix between input and output parameters of the PSS data set

Subsequently, the database is partitioned into two subsets: training and testing parts. The former serves as the platform for constructing and optimizing the ML model, while the latter functions as the arena for assessing the model's performance. As conventionally practiced, a 70% allocation to the training set and a 30% allocation to the testing set is adhered to [31].

3. Methods

3.1. Machine learning methods

3.1.1. Gradient Boosting (GB) method

GB [32] is a powerful and versatile ML technique that has gained prominence for its effectiveness in predictive modeling and regression analysis. It belongs to the ensemble learning family of algorithms, where multiple weak learners (often simple decision trees) are combined to create a robust and accurate predictive model.

The fundamental idea behind GB is to iteratively build a series of weak models, each correcting the errors of its predecessor. This is achieved by assigning weights to the data points based on the errors made by the previous models. The algorithm aims to optimize a loss function, gradually reducing the residuals and improving the overall predictive accuracy. It is widely used in various applications, including regression, classification, and ranking tasks, and has proven to be highly effective in producing accurate and robust predictions.

3.1.2. Optimization techniques

a. Grid Search Optimization

Grid Search Optimization is a systematic and exhaustive hyperparameter tuning technique widely used in ML to find a model's optimal set of hyperparameters. Hyperparameters are external configurations not learned from the data but influence the learning process. They include parameters like learning rate, regularization strength, or the number of hidden layers in a neural network.

The Grid Search Optimization technique defines a grid of hyperparameter values to be explored. The model is trained and evaluated using a chosen performance metric for each combination of hyperparameter values in the grid. The combination of hyperparameters that yields the

best performance according to the metric is then selected as the optimal configuration. While Grid Search Optimization ensures a thorough exploration of the hyperparameter space, it can be computationally expensive, particularly with numerous hyperparameters or a broad range of values. Nonetheless, it remains a fundamental and widely used technique, providing a robust approach to hyperparameter tuning and enhancing model performance across various domains and algorithms.

b. Random Search Optimization

Random Search Optimization is an ML hyperparameter tuning technique that deviates from the systematic approach of Grid Search. In contrast to the exhaustive exploration of all possible combinations, Random Search selects hyperparameter configurations by random sampling within predefined search space ranges or distributions. This method aims to efficiently discover effective hyperparameter settings while requiring fewer computational resources than Grid Search.

In Random Search, each set of hyperparameter values is randomly chosen and used to train and evaluate a model. Like Grid Search, this process involves fitting the model to the training data, validating on a separate dataset, and assessing performance using a designated metric. The randomness in selecting hyperparameter configurations allows Random Search to explore the hyperparameter space efficiently, potentially identifying effective configurations more swiftly than exhaustive search methods.

One of the advantages of Random Search is its resource efficiency, as it does not require evaluating every possible combination. This makes it particularly beneficial in situations where computational resources are limited. Although Random Search does not guarantee finding the absolute optimal configuration, it has demonstrated practical effectiveness, especially in scenarios with large and complex search spaces.

3.2. Performance indices of models

In this study, the estimating results of the GB model are assessed using commonly employed statistical criteria, specifically, the root mean square error (RMSE), the mean absolute error (MAE), and the coefficient of determination (R^2). These criteria are pivotal in regression analysis, elucidating the relationship between predicted output and actual values in various ways. A higher R^2 value indicates a strong correlation, whereas lower values of RMSE and MAE signify better model performance. The following formulas determine these criteria:

$$RMSE = \sqrt{\frac{1}{N}\sum_{k=1}^{N}\left(p_k - q_k\right)^2} \quad (1)$$

$$MAE = \frac{1}{N}\sum_{k=1}^{N}\left|p_k - q_k\right| \quad (2)$$

$$R^2 = 1 - \left[\frac{\sum_{k=1}^{N}\left(p_k - q_k\right)^2}{\sum_{k=1}^{N}\left(p_k - \bar{p}_k\right)^2}\right] \quad (3)$$

where N is the number of database, q is the predicted value and p is the actual value.

4. Results and Discussion

4.1. Hypeparameter tuning

Hyperparameter optimization stands as a pivotal undertaking in the construction of ML models, serving the purpose of pinpointing the most favorable hyperparameter values to enhance the model's predictive capabilities on a given dataset. ML models undergoing hyperparameter optimization often exhibit heightened accuracy and robustness, surpassing those without such fine-tuning. Within the scope of this study, two distinct techniques, namely grid search (Grid.S) and random search (Ran.S), are employed to fine-tune the hyperparameters of the GB model. Four particularly influential hyperparameters, as outlined by reference [33], are selected for optimization:

- Learning rate (L.R): This hyperparameter governs the magnitude of steps taken

during the optimization procedure, dictating the size of the value incorporated into the model at each step to enhance predictive quality.

- Max depth (M.D): M.D regulates the maximum depth attainable by decision trees within the model.
- n_estimator (Ne): Ne plays a pivotal role in determining the quantity of decision trees generated within the model.
- min_samples_leaf (M.S.L): M.S.L establishes the minimum count of data points obligatory within each decision tree leaf.

In-depth exploration and fine-tuning of these influential hyperparameters enhance the capacity to harness ML techniques effectively in solving complex problems across various domains. The hyperparameter search space is defined based on suggestions from previous research [34–36] and initial experiments, and presented in Table 2. The remaining hyperparameters of the GB model adhere to the default Python settings in this study. Hyperparameter tuning and model assessment are conducted utilizing a five-fold cross-validated dataset to augment the correlation between experimental and predicted outcomes. The coefficient of determination is adopted to gauge model performance during optimization.

In adherence to the grid search methodology, a systematic amalgamation of 1200 hyperparameter sets yields an equivalent number of corresponding GB models. In parallel, the random search strategy conducts 900 searches to ascertain the most fitting hyperparameter set, mirroring the outcomes derived from the grid search. The evaluation entails a comprehensive examination of model performance, encompassing factors such as predictive accuracy, stability, and alignment with experimental data. This rigorous assessment leads to the identification of the top 10 GB models, collectively representing the most adept and refined configurations. Notably, the performance evaluation is based on the R^2 criterion, with the outcomes meticulously arranged in descending order and presented in Table 3. The results of this hyperparameter optimization process bear significance in ML as they lay the groundwork for selecting the most adept GB models. These optimized models, guided by refined hyperparameters, offer enhanced predictive capabilities and exhibit superior alignment with experimental data.

Fig. 3 provides a visual representation of the R^2 values and the average runtime associated with the top 10 models that have undergone hyperparameter optimization using grid and random search techniques. Concurrently, Table 3 offers insights into the overall runtime for both optimization methods. Notably, within the framework of random search, which involves 900 systematic inquiries, the optimal hyperparameter set is successfully identified. This achievement aligns closely with the outcomes derived from grid search but stands out for its notably reduced runtime. However, it is important to acknowledge that determining the precise number of searches necessitates empirical experimentation and hinges upon the specific hyperparameter configuration. The exploration of diverse optimization techniques, as exemplified by Model 1 (GB_01), showcases its potential to yield robust predictive results for PSS of two-way slabs.

4.2. Prediction results of PSS of two-way slab according to the best GB model

To ascertain the robustness and applicability of the GB_01 models, a Monte Carlo simulation (MCS) technique is harnessed. This method generates multiple distinct training and testing datasets, thereby ensuring the model's reliability and generalizability. The convergence values, denoting the model's stability and generalization, are observed over a series of Monte Carlo simulations conducted within a predefined range around the average convergence values. It is worth highlighting that an increase in the number of

Monte Carlo simulations correlates with an extended convergence rate for the models, leading to elongated training durations and heightened problem complexity. The utilization of the Monte Carlo simulation technique plays a pivotal role in affirming the reliability and versatility of the GB_01 models. These models are not merely designed to perform well on specific datasets but are engineered to exhibit robust performance across various scenarios and datasets.

Two evaluation criteria, namely R^2 and RMSE, play a crucial role in gauging the influence of the number of Monte Carlo simulations (MCS) on the convergence results. Fig. 4 visually represents the normalized convergence outcomes for R^2 and RMSE concerning training and testing datasets. In this graphical representation, the horizontal axis signifies the count of MCS, while the vertical axis depicts the normalized convergence values related to the evaluation criteria. Notably, for the R^2 criterion, the validation dataset requires a minimum of 130 MCS to attain a convergence range of ±0.03% around the average value. In contrast, the training dataset reaches this range within ±0.01% around the average value after the initial simulation. Regarding the RMSE criterion, the training dataset achieves convergence within ±0.1% of the range following the first simulation, while the validation dataset necessitates approximately 106 MCS to reach the convergence limit of ±0.5%. These findings advocate the recommendation of employing 200 MCS to ensure the assessment of model convergence, thereby validating the reliability of predictions generated by the GB model and confirming its generalizability. The significance of these results resides in their capacity to ensure the performance and generalizability of the GB model across diverse datasets.

This section presents a typical prediction outcome generated by the GB model across 200 simulations. Regression plots for both the training and testing segments are showcased in Fig. 5, with the horizontal axis denoting experimental values and the vertical axis representing predicted output values. These plots reveal the presence of robust linear regression lines between experimental and predicted values, yielding notably high R^2 values of 0.998 and 0.988 for the training and testing segments, respectively. These metrics validate the model's precision and reliability in effectively capturing the intricate relationship between input parameters and the PSS.

A comprehensive assessment of performance metrics, encompassing RMSE and MAE, reinforces the model's accuracy, with low error values of 24.995 kN and 3.425 kN observed for the training part, and 32.615 kN and 24.230 kN for the testing part, respectively. The model consistently exhibits exemplary performance across these diverse metrics, further underscoring its robustness and aptitude for predicting the PSS of two-way slabs. Moreover, Fig. 6a and 6b present charts and cumulative error distributions between predicted and experimental PSS values for both datasets, offering a holistic view of the model's predictive capabilities. Additionally, Table 4 provides quantitative values for the model's performance evaluation criteria. It becomes evident that the application of the GB_01 model to predict the PSS of two-way slabs attains an elevated level of accuracy, thereby mitigating the need for extensive experimental efforts and preserving valuable resources.

The paramount importance of these results lies in their collective affirmation of the GB_01 model's reliability and precision in predicting PSS. The model's capability to consistently produce accurate predictions across various evaluation metrics signifies its potential as a valuable tool for structural engineers and researchers in two-way slab design and analysis.

4.3. Comparison with design codes

In this section, the predictive performance of the GB_01 model is assessed in comparison to established standards used to determine the PSS

of two-way slabs. Four standard codes are provided for comparison purposes, including ACI 318-08 [7], CEB-FIP-90 [9], BS 8110-97 [8], and EC 2 [10]. Table 5 presents a detailed overview of the equations derived from the selected design codes for predicting PSS in two-way slabs. The comparative analysis highlights the alignment and variations between the predictions generated by the GB_01 model and those obtained from the established standards.

Table 6 presents the comparative results considering three previously defined metrics. The findings reveal that ACI 318-08 exhibits the least accuracy among the design codes examined when applied to the collected dataset. This is evident through the RMSE of 193.4 kN, MAE of 118.9 kN, and an R^2 value of 0.928. Conversely, CEB-FIP-90, BS 8110-97, and EC2 demonstrate greater accuracy in predicting PSS than ACI, with RMSE values ranging from 80 to 88 kN, MAE values from 44 to 56 kN, and R^2 values hovering around 0.98. Notably, the employment of the AI-based GB model showcases remarkable accuracy, with an RMSE of 27.5 kN, MAE of 9.7 kN, and an impressive R^2 of 0.99.

These results underline the substantial disparities in predictive accuracy between the different design codes. ACI falls short in providing accurate PSS predictions, with relatively higher errors than CEB-FIP, BS, and EC2. The superior performance of the GB model highlights the potential of artificial intelligence in enhancing the precision of PSS predictions. This advances structural engineering practices and underscores the critical role of ML models in augmenting the reliability of design processes and ensuring the safety of construction projects. Further exploration and validation of AI models like the GB model hold significant promise for future structural engineering applications.

4.4. Parametric study

A parametric study is presently undertaken to assess input variations' impact and influence on PSS. In this study, the baseline input considered is the slab thickness, with an examination of slab thickness in conjunction with other pertinent input factors. The results of this analysis are visually represented in Fig. 7. It serves as a graphical representation of the outcomes obtained from the parametric study. It provides a visual insight into the influence of varying input parameters, with a specific focus on slab thickness, on the PSS of the structural elements under consideration.

In examining the variation in parameter C, ranging from 80 to 520 mm, it is observed that PSS exhibits a broad spectrum, spanning from 250 to 1220 mm. Nevertheless, the overall trend remains relatively constrained, with minimal alterations for fixed values of h. When considering the range of h from 20 to 170, a gradual shift in PSS is discernible, progressing from 250 to 400. A notable escalation in PSS becomes evident when h is extended from 170 to 370, resulting in a PSS increase from 400 to 1150. Beyond the threshold h value of 370, PSS stabilizes and shows only slight variations around 1200. These observations reaffirm the significance of h as a substantial input parameter in the context of PSS, with its variations eliciting notable changes in structural response. The findings underscore the importance of considering h as a critical factor in the design and assessment of structural elements, as it significantly influences PSS and, consequently, the overall structural integrity.

The fluctuation in parameter d exhibits a similarity to the influence of C concerning its impact on PSS. As d undergoes variation within the range of 35 to 500 mm, PSS exhibits considerable fluctuations, ranging from 100 to 2500. However, it's worth noting that these variations are primarily driven by the influence of h. Specifically, when d assumes a smaller value, such as d=35 mm, PSS demonstrates a notably higher magnitude than the increased values of d. Conversely, an increment in d from 79 to 500 mm has a relatively minimal impact on PSS. The patterns of PSS changes in this scenario closely resemble those observed for

variable C, with two noteworthy thresholds identified at approximately 170 and 370 mm.

A similar parametric investigation extends to the parameters rho, fc, and fy, encompassing a comprehensive examination of their effects on PSS. Remarkably, a consistent pattern emerges across all cases, revealing the presence of two pivotal thresholds at approximately 170 and 370 mm for h. When considering rho, with a range from 0.25 to 5.01, PSS exhibits changes ranging from 200 to 1500 kN. A parallel analysis of fc within the 12.3 to 19 MPa range demonstrates PSS fluctuations ranging from 180 to 1500 kN. In contrast, varying fy from 294 MPa to 720 MPa results in PSS changes from 150 to 1300 kN. Notably, the influence of fy is comparatively modest when juxtaposed with fc. Conversely, the variation in rho yields limited changes in PSS, as for any given rho value, PSS varies by only 200 kN. However, it is essential to acknowledge that higher values of h can induce more substantial PSS fluctuations, with variations in rho potentially resulting in changes of approximately 500 kN.

These findings emphasize the intricate interplay between structural parameters rho, fc, fy, and h, further corroborating the significance of h as a critical governing factor in PSS. Establishing consistent thresholds at 170 and 370 mm for h underscores the importance of these values in optimizing structural performance. The insights gained from this comprehensive parametric study provide structural engineers with valuable guidance for enhancing the precision and reliability of structural design practices. Additionally, recognizing the varying degrees of influence exerted by rho, fc, and fy on PSS offers valuable information for tailoring structural designs to meet specific performance requirements.

Table 2. Search domain and default values of hyperparameters in the GB model

n_estimators (N.S)	**Learning rate (L.R)**	**Max depth (M.D)**	**min_samples_leaf (M.S.L)**
100-1000	0.1-0.5	3-8	1-4
loss	**subsample**	**criterion**	**min_samples_split**
squared_error	1	friedman_mse	2

Table 3. Optimal hyperparameters of GB models

Hyper parameter	**L.R**	**M.D**	**M.S.L**	**N_e**	**R^2_{cv}**	**L.R**	**M.D**	**M.S.L**	**N_e**	**R^2_{cv}**
Optimization techniques	**Grid search CV (Grid.S)**					**Random search CV (Random.S)**				
GB_01	**0.1**	**5**	**3**	**200**	**0.981327**	**0.1**	**5**	**3**	**200**	**0.981327**
GB_02	0.1	5	3	300	0.980792	0.1	6	3	200	0.980699
GB_03	0.1	6	3	200	0.980699	0.1	5	3	400	0.980666
GB_04	0.1	5	3	400	0.980666	0.1	8	3	200	0.980035
GB_05	0.1	5	3	500	0.980587	0.1	5	3	900	0.980541
GB_06	0.1	5	3	600	0.980573	0.1	5	3	1000	0.980471
GB_07	0.1	5	3	700	0.980546	0.1	4	3	200	0.980429
GB_08	0.1	8	3	200	0.980541	0.1	6	3	200	0.980300
GB_09	0.1	5	3	800	0.980510	0.1	8	3	100	0.980268
GB_10	0.1	5	3	900	0.980471	0.1	8	1	300	0.980255
Total run time (s)	1842.818					713.710				

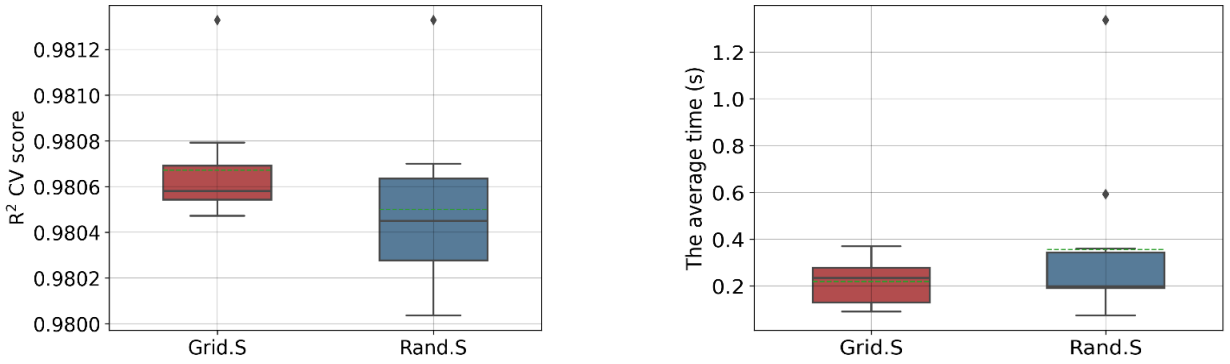

Fig. 3. Box plot represents the R^2 criterion value and average running time of the 10 best model

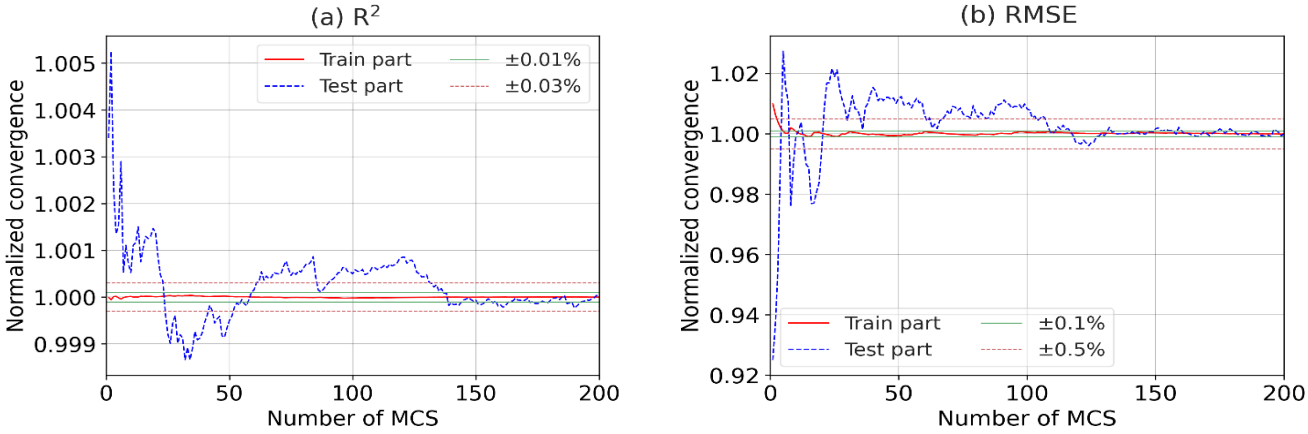

Fig. 4. Evaluate the convergence level of the GB model according to R^2 and RMSE criteria

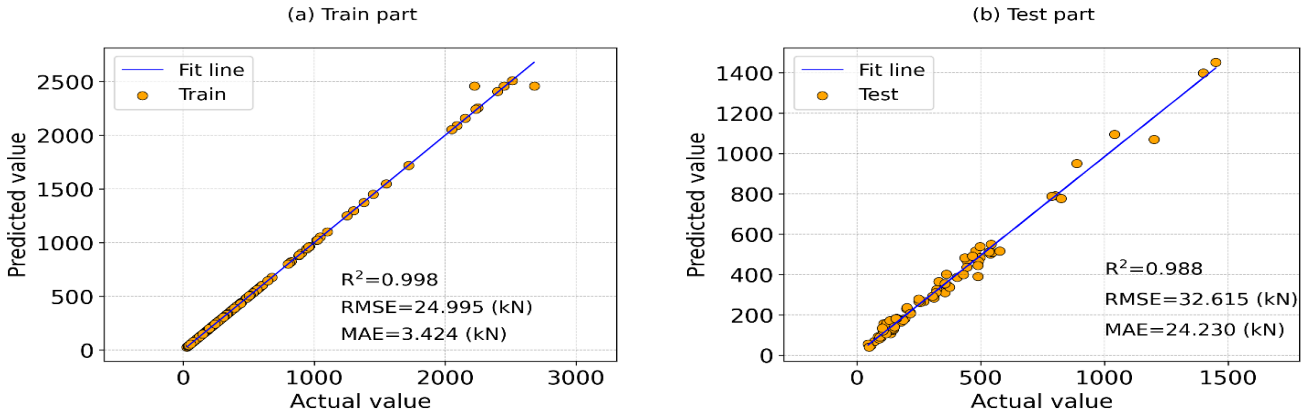

Fig. 5. Correlation analysis between actual and predicted values (a) train part and (b) test part

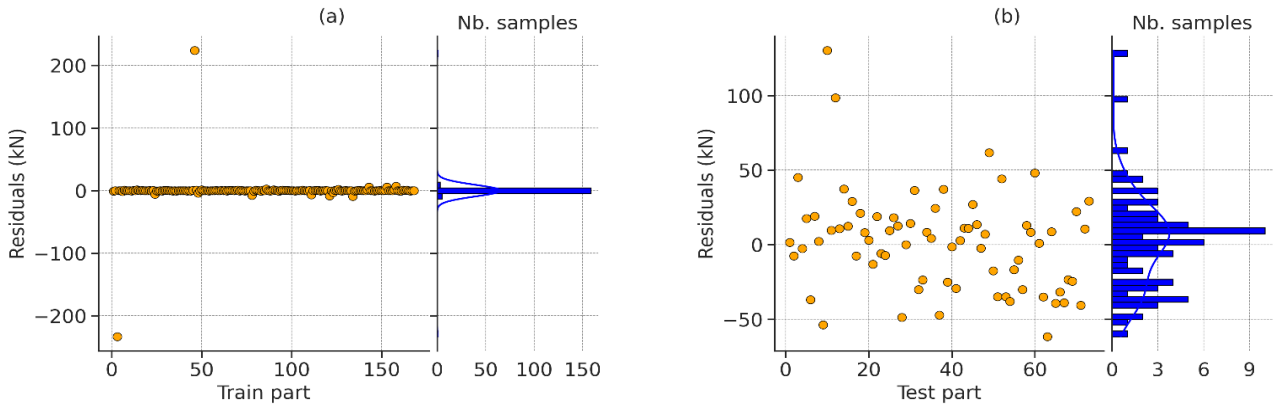

Fig. 6. Error between PSS prediction results and the actual values (a) train part, (b) test part

Table 4. Values of statistical criteria describing GB_01 model performance

	RMSE (kN)	MAE (kN)	R^2
Train part	24.995	3.424	0.998
Test part	32.615	24.230	0.988
All data	27.527	9.727	0.997

Table 5. Equations of standard codes

Models	Equation
ACI 318-08 [7]	$V_n = \min(V_{n1}, V_{n2}, V_{n3})$ $V_{n1} = 0.083\left(2 + \frac{4}{\beta_c}\right)\lambda\sqrt{f_c}b_0 d,$ $V_{n2} = 0.083\left(2 + \alpha_s \frac{d}{b_0}\right)\lambda\sqrt{f_c}b_0 d,$ $V_{n3} = 0.33\lambda\sqrt{f_c}b_0 d$ where b_0: the perimeter of the critical section (mm), d: the effective depth of the slab (mm), β_c: the ratio of the longer to the shorter dimension of the loaded area, f_c: the cylinder compressive strength of concrete (MPa), λ = 1, α_s = 40
CEB-FIP-90 [9]	$V_n = 0.18 b_0 d \times \xi \times \sqrt[3]{100 \times \rho \times f_{ck}}$ $\xi = 1 + \sqrt{200/d}$ where f_{ck}: the characteristic cylinder compressive strength (MPa), ρ: the ratio of flexure reinforcement.
BS 8110-97 [8]	$V_n = 0.79 \times \sqrt[3]{100 \times \rho}\sqrt[4]{400/d} \times \sqrt[3]{f_{cu}/25} \times \frac{b_0 d}{1.25}$ where f_{cu}: the cubic compressive strength (MPa).
EC 2 [10]	$V_u = \frac{0.18}{\gamma_c} K b_0 d (100 \times \rho \times f_{ck})^{1/3} \frac{2d}{a_{crt}} \geq 0.035 K^{3/2} f_{ck}^{1/2} \frac{2d}{a_{crt}} b_0 d$ where: γ_c = 1.5, $K = 1 + \sqrt{200/d} \leq 2$ a_{crt}: the distance from column face to the control perimeter

Table 6. Statistical criteria values of design codes in predicting the PSS of two-way slabs

Models	Criteria		
	RMSE (kN)	MAE (kN)	R^2
ACI 318-08 [7]	193.445	118.940	0.928
CEB-FIP-90 [9]	80.823	44.893	0.988
BS 8110-97 [8]	81.725	45.634	0.987
EC 2 [10]	88.493	56.140	0.986
This study	27.527	9.727	0.997

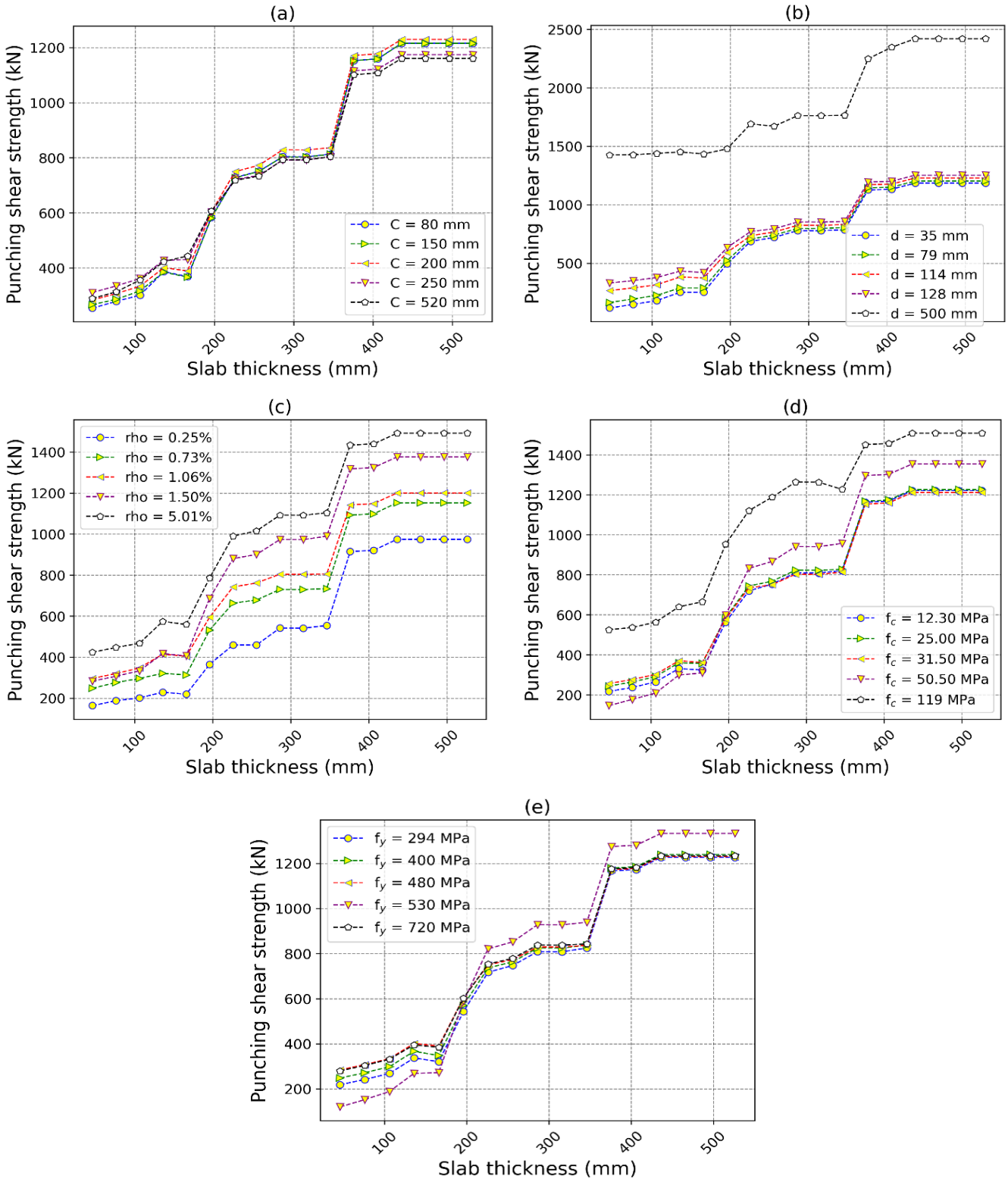

Fig. 7. Parametric study for PSS considering the slab thickness and other input parameters: (a) width of column, (b) effective depth of column, (c) reinforcement ratio, (d) compressive strength of concrete, and (e) yield strength of steel

5. Conclusion

In conclusion, this study harnesses ML, specifically a GB model, to predict the PSS of two-way reinforced concrete flat slabs. The research showcases the model's remarkable accuracy in capturing the intricate relationships between input

parameters and PSS. Key findings include R^2 values of 0.998 and 0.988 for the training and testing segments, respectively, alongside low error values (RMSE and MAE) for both parts. These metrics affirm the GB model's precision, reliability, and robustness in predicting PSS, thus reducing the need for resource-intensive experimental endeavors.

While this research represents a significant advancement in structural engineering and ML, several avenues for future exploration emerge. First, expanding the dataset to include a wider range of parameters and structural variations could enhance the model's versatility and generalizability. Exploring advanced ML techniques and ensembles may also lead to even more accurate predictions. Lastly, investigating real-time monitoring and sensor data integration into the model for ongoing structural assessment and safety analysis is an exciting prospect. These future endeavors hold the potential to revolutionize the field of structural analysis and design, offering efficient and accurate tools for engineers and researchers.

Conflict of Interest: The authors declare no conflict of interest.

Funding: This research did not receive any specific grant from the public, commercial, or not-for-profit funding agencies.

Availability of data and material: Data will be made available on request.

Reference

[1]. M. Adom-Asamoah, C.K. Kankam. (2008). Behaviour of reinforced concrete two-way slabs using steel bars milled from scrap metals. *Materials & Design*, 29(6), 1125-1130.

[2]. R.C. Elstner, E. Hognestad. (1956). Shearing strength of reinforced concrete slabs. *Journal Proceedings*, 53(7), 29-58.

[3]. J. Moe. (1961). Shearing strength of reinforced concrete slabs and footings under concentrated loads. *Portland Cement Association, Research and Development Laboratories*. Skokie, Ill.

[4]. R.D. Mowrer, M.D. Vanderbilt. (1967). Shear strength of lightweight aggregate reinforced concrete flat plates. J*ournal Proceedings*, 64(11), 722-729.

[5]. P.E. Regan. (1986). Symmetric punching of reinforced concrete slabs. *Magazine of Concrete Research*, 38(136), 115-128.

[6]. S. Guandalini, O. Burdet, A. Muttoni. (2009). Punching tests of slabs with low reinforcement ratios. *ACI Structural Journal*, 106(1), 87-95.

[7]. A.C.I. Committee. (2005). Building code requirements for structural concrete (ACI 318-08) and commentary (ACI 318R-08). *American Concrete Institute*. USA.

[8]. AISC. (2016). Specification for structural steel buildings ANSI/AISC 360–16. *American Institute of Steel Construction, Chicago*. USA.

[9]. J.C. Walraven. (2012). Model Code 2010-Final Draft: Volume 1. *The International Federation for Structural Concrete FIB*. ISBN: 978-2-88394-095-6.

[10]. Australian Standard. (2004). W. AS5100, Bridge design, Part 6: steel and composite construction.

[11]. A.T.C. Goh. (1995). Empirical design in geotechnics using neural networks. *Geotechnique*, 45(4), 709-714.

[12]. B.T. Pham, M.D. Nguyen, D. Van Dao, I. Prakash, H.-B. Ly, T.-T. Le, L.S. Ho, K.T. Nguyen, T.Q. Ngo, V. Hoang. (2019). Development of artificial intelligence models for the prediction of Compression Coefficient of soil: An application of Monte Carlo sensitivity analysis. *Science of The Total Environment*, 5, 172-184, 116915.

[13]. H.-B. Ly, E. Monteiro, T.-T. Le, V.M. Le, M. Dal, G. Regnier, B.T. Pham. (2019). Prediction and sensitivity analysis of bubble dissolution time in 3D selective laser sintering using ensemble decision trees. *Materials*, 1544.

[14]. Q.H. Nguyen, H.-B. Ly, V.Q. Tran, T.-A. Nguyen, V.-H. Phan, T.-T. Le, B.T. Pham. (2020). A novel hybrid model based on a

feedforward neural network and one step secant algorithm for prediction of load-bearing capacity of rectangular concrete-filled steel tube columns. *Molecules*, 25(15), 3486.

[15]. H.Q. Nguyen, H.-B. Ly, V.Q. Tran, T.-A. Nguyen, T.-T. Le, B.T. Pham. (2020). Optimization of artificial intelligence system by evolutionary algorithm for prediction of axial capacity of rectangular concrete filled steel tubes under compression. *Materials*, 13(5), 1205.

[16]. H.-B. Ly, T.-T. Le, L.M. Le, V.Q. Tran, V.M. Le, H.-L.T. Vu, Q.H. Nguyen, B.T. Pham. (2019). Development of hybrid machine learning models for predicting the critical buckling load of I-shaped cellular beams. *Applied Sciences*, 9(24), 5458.

[17]. H.-B. Ly, L.M. Le, H.T. Duong, T.C. Nguyen, T.A. Pham, T.-T. Le, V.M. Le, L. Nguyen-Ngoc, B.T. Pham. (2019). Hybrid artificial intelligence approaches for predicting critical buckling load of structural members under compression considering the influence of initial geometric imperfections. *Applied Sciences*, 9(11), 2258.

[18]. D.V. Dao, H.-B. Ly, S.H. Trinh, T.-T. Le, B.T. Pham. (2019). Artificial intelligence approaches for prediction of compressive strength of geopolymer concrete. *Materials*, 12(6), 983.

[19]. T.-A. Nguyen, H.-B. Ly, H.-V.T. Mai, V.Q. Tran. (2020). Prediction of Later-Age Concrete Compressive Strength Using Feedforward Neural Network. *Advances in Materials Science and Engineering*, 89.

[20]. T.-A. Nguyen, H.-B. Ly, B.T. Pham. (2020). Backpropagation Neural Network-Based Machine Learning Model for Prediction of Soil Friction Angle. *Mathematical Problems in Engineering*, 5, 1-11.

[21]. H.-B. Ly, T.-A. Nguyen, B.T. Pham. (2021). Estimation of Soil Cohesion Using Machine Learning Method: A Random Forest Approach. *Advances in Civil Engineering*, 1-14.

[22]. D.V. Dao, A. Jaafari, M. Bayat, D. Mafi-Gholami, C. Qi, H. Moayedi, T.V. Phong, H.-B. Ly, T.-T. Le, P.T. Trinh. (2020). A spatially explicit deep learning neural network model for the prediction of landslide susceptibility. *Catena*, 188, 104451.

[23]. V.-T. Nguyen, T.H. Tran, N.A. Ha, V.L. Ngo, A.-A. Nadhir, V.P. Tran, H. Duy Nguyen, M. MA, A. Amini, I. Prakash. (2019). GIS based novel hybrid computational intelligence models for mapping landslide susceptibility: a case study at Da Lat city, Vietnam. *Sustainability*, 11(24), 7118.

[24]. N.-D. Hoang. (2019). Estimating punching shear capacity of steel fibre reinforced concrete slabs using sequential piecewise multiple linear regression and artificial neural network. *Measurement*, 137, 58-70.

[25]. A.A. Elshafey, E. Rizk, H. Marzouk, M.R. Haddara. (2011). Prediction of punching shear strength of two-way slabs. *Engineering Structures*, 33(5), 1742-1753.

[26]. M. Grira. (1990). A critical review of the symmetric punching shear of reinforced concrete flat slabs. *University of Ottawa*. Canada.

[27]. G. Rankin, A. Long. (1987). Predicting the punching strength of conventional slab-column specimens. *Proceedings of the Institution of Civil Engineers*, 82(2), 327-346.

[28]. N.J. Gardner. (1990). Relationship of the punching shear capacity of reinforced concrete slabs with concrete strength. *Structural Journal*, 87(1), 66-71.

[29]. D.D. Magura, W.G. Corlet. (1971). Tests to Destruction of a Multipanel Waffle Slab Structure-1964-1965 New York's World Fair. *Journal Proceedings*, 68(9), 699-703.

[30]. D. Yitzhaki. (1966). Punching strength of reinforced concrete slabs. *Journal Proceedings*, 63(5), 527-542.

[31]. T. Hastie, R. Tibshirani, J.H. Friedman, J.H. Friedman. (2009). The elements of statistical learning: data mining, inference, and prediction.

Springer.

[32]. A. Natekin, A. Knoll. (2013). Gradient boosting machines, a tutorial. *Frontiers in Neurorobotics*, 7, 21.

[33]. A. Shatnawi, H.M. Alkassar, N.M. Al-Abdaly, E.A. Al-Hamdany, L.F.A. Bernardo, H. Imran. (2022). Shear Strength Prediction of Slender Steel Fiber Reinforced Concrete Beams Using a Gradient Boosting Regression Tree Method. *Buildings*, 12(5), 550.

[34]. B.N. Phung, T.-H. Le, T.-A. Nguyen, H.-B. Ly. (2023). Advancing basalt fiber asphalt concrete design: A novel approach using gradient boosting and metaheuristic algorithms. *Case Studies in Construction Materials*, 19, e02528.

[35]. H.-B. Ly, T.-A. Nguyen. (2023). Accelerating fluid flow simulations through doubly porous media using a FEM-assisted machine learning approach. *Results in Physics*, 54, 107036.

[36]. B.-N. Phung, T.-H. Le, M.-K. Nguyen, T.-A. Nguyen, H.-B. Ly. (2023). Practical Numerical Tool for Marshall Stability Prediction Based On Machine Learning: An Application for Asphalt Concrete Containing Basalt Fiber. *Journal of Science and Transport Technology*, 3(3), 27-45.